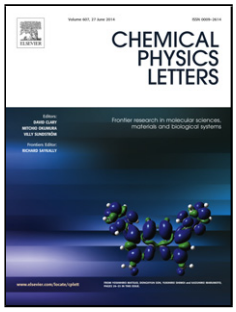

Title: In vitro monitoring of ring opening of leflunomide: A Surface Enhanced Raman Scattering and DFT based approach

Author: Poornima Sharma Debraj Gangopadhyay Pushkar Singh P.C. Mishra Volker Deckert Jürgen Popp Ranjan K. Singh

PII: S0009-2614(14)00750-7
DOI: http://dx.doi.org/doi:10.1016/j.cplett.2014.08.068
Reference: CPLETT 32460

To appear in:

Received date: 7-8-2014
Revised date: 26-8-2014
Accepted date: 27-8-2014

Please cite this article as: P. Sharma, D. Gangopadhyay, P. Singh, P.C. Mishra, V. Deckert, J. Popp, R.K. Singh, In vitro monitoring of ring opening of leflunomide: A Surface Enhanced Raman Scattering and DFT based approach, *Chem. Phys. Lett.* (2014), http://dx.doi.org/10.1016/j.cplett.2014.08.068

Highlights

- Surface enhanced Raman scattering based in vitro reaction monitoring.
- Leflunomide ring opening at pH ~10 to form metabolite A771726.
- Correlation of experimental results with transition state calculations using DFT.
- Role of catalytic OH^- ions in ring opening reaction by SERS and DFT calculations.
- Effect of different basic catalysts on reaction barrier energy.

***Graphical Abstract (pictogram) (for review)**

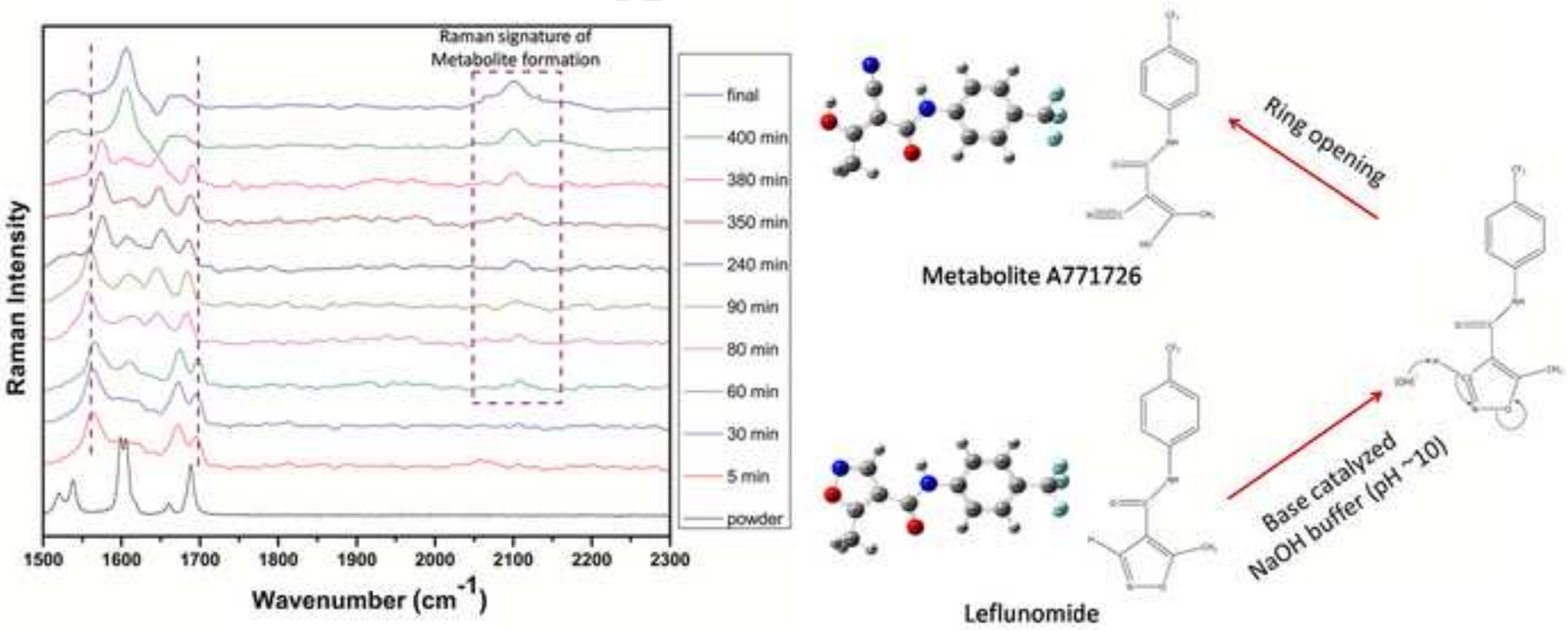

In vitro monitoring of ring opening of leflunomide: A Surface Enhanced Raman Scattering and DFT based approach

Poornima Sharma[1], Debraj Gangopadhyay[1], Pushkar Singh[2], P. C Mishra[1], Volker Deckert[2,3], Jürgen Popp[2,3] and Ranjan K. Singh[1]

[1]Department of Physics, Banaras Hindu University, Varanasi-221005, India.

[2]Leibniz Institute of Photonic Technology, Albert-Einstein-Straße 9, 07745 Jena, Germany.

[3]Institute of Physical Chemistry and Abbe Center of Photonics, Friedrich-Schiller University, Jena, Helmholtzweg 4, 07743 Jena, Germany.

Abstract

The in vitro mechanism of ring opening of leflunomide resulting in formation of a metabolite A771726 has been studied by time series surface enhanced Raman spectra using NaOH buffer at pH ~10. The decomposition of leflunomide into A771726 through N-O bond cleavage was identified by the Raman signature of C≡N bond of A771726. The experimental results have been correlated with theory by transition state calculations of the reaction using different basic catalysts; OH^-, formate and formate +water and water alone. The reaction barrier energy is found to be lowest with OH^- as a catalyst.

Keywords: *leflunomide; A771726; Ring opening; metabolism; SERS; DFT*

[*]**Correspondence to:** Prof. Ranjan Kumar Singh, Department of Physics, Banaras Hindu University, Varanasi-221005, India. E-mail: ranjanksingh65@rediffmail.com, Phone No : +915426701569; Fax No.: +915422368390

1. Introduction

Leflunomide [N-{(4-Trifluoromethyl)phenyl}-5-methylisoxazole-4-carboxamide] is a disease modifying rheumatoid arthritis drug that inhibits de novo pyrimidine nucleotide synthesis by blocking the dihydroorotate dehydrogenase (DHODH) enzyme [1-3]. Its tyrosine kinase inhibiting activity also permits it to act as an anticancer drug [4, 5]. Leflunomide belongs to class II of the biopharmaceuticals classification system (BCS) because of its poor solubility in water (less than 40 mg/L). The oral intake of leflunomide in human body leads to the formation of its active α-cyanoenol metabolite A771726 [2-cyano-3-oxo-N-{(4-trifluoromethyl)phenyl}butyramide] or teriflunomide [6]. Many isoxazole ring containing drugs including leflunomide have been reported to undergo extensive reductive ring opening, leading to formation of imine intermediates [7-9]. The biotransformation of leflunomide to its active metabolite A771726 by isoxazole ring opening is an important reaction, since this metabolite is responsible for the anti-infalammatory and disease-modifying properties of leflunomide [3]. In isoxazole ring the higher electronegativity of oxygen atom adjacent to the nitrogen atom is important cause for N-O bond cleavage [10]. The substitution and unsubstitution of the H atom attached to C3 atom in isoxazole ring plays an important role in such reactions. Two pathways have been suggested in the literature for ring opening in isoxazoles. The first pathway is for the molecules with the C3 substituted isoxazole, where two electron reductive cleavage of N-O bond is involved [11-12]. The second pathway is suitable for the C3 unsubstituted isoxazole (leflunomide), where this mechanism occurs via deprotonation of the C3 site followed by N-O bond cleavage [13]. Kalgutkar et al. [6] have reported that this biotransformation from Leflunomide to A771726 is either enzymatic or non-enzymatic (basic) and the two factors responsible for the decomposition of leflunomide to A771726 are pH and temperature. They reported that leflunomide favoured ring opening at basic pH (10) and this base catalyzed reaction is faster at 37°C. A molecular modelling study of leflunomide, its active metabolite and metabolite analogues has been reported by Panek et al. [14]. They reported that intramolecular proton transfer is preferred in the polar environment. Stability, crystal structure and polymorphic forms of Leflunomide have been reported by Vega et al. [15].

In the present work, we have investigated the second pathway to study the ring opening of leflunomide i.e. a base catalyzed reaction. Recent advancements in Raman spectroscopic techniques have led to detailed understanding of several reaction mechanisms [16-19]. Surface enhanced Raman scattering (SERS) is an analytical technique which uses

the exciting optical properties of metallic nanostructures and resulting enhancement in Raman signals when the target molecules are attached to metallic (Ag, Au) nanostructures [20-22]. Due to high sensitivity and reproducibility, SERS active substrate can be used for studying biologically relevant processes [23, 24]. In the present work, we have for the first time studied the ring opening reaction of leflunomide and monitored the metabolic process thoroughly with the help of SERS and Transition state calculations. The precise understanding of the process at molecular level which has been achieved through this work will be very useful for further spectroscopic and pharmacological studies.

2. Computational Details

Molecular geometries of leflunomide and its active metabolite A771726 in gas phase were fully optimized. Geometry of the transition state (TS) between leflunomide and A771726 was also optimized. The density functional theoretical (DFT) method having Becke's non local three-parameter exchange and correlation functional along with the Lee-Yang-Parr correctional functional (B3LYP) [25, 26] was employed for the calculations. Vibrational analysis was performed in order to make sure that each total energy extremum obtained was genuine, i.e. each minimum has all real frequencies and each transition state has only one imaginary frequency. Zero-point energy (ZPE) correction to total energy and thermal energy correction to enthalpy were obtained at the B3LYP/6-311++g(d,p) level of theory in gas phase and these corrections were also considered to be valid for the corresponding single point energy calculations performed at same level of theory. All the calculations were performed by Gaussian 03 [27] program. For visualization of the optimized structures and vibrational modes Gauss View 4.1 [28] program was used.

2.1 Experimental details

Leflunomide purchased from Bio-trends (Germany) was used without any further purification. The experimental setup has been described in detail elsewhere [29]. In brief, laser was focused by an oil immersion microscope objective (40X, 1.35NA, Olympus) on a silver island film. The silver film was prepared by evaporation of silver [30]. The scattered SERS signal from leflunomide is collected with the same objective and passed through a dichroic mirror and notch filter and finally entered the spectrometer (Action Advanced SP2750 A, SI GmbH, Germany). All measurements are performed with a 532 nm laser at 150 μW power.

Raman spectroscopy is capable of tracking the changes at molecular level in the course of the reaction. However, the monitoring requires the reaction to take place in aqueous

solution. The poor solubility of leflunomide in water restricted us to use an extremely dilute (10^{-4} M) aqueous solution. Linear Raman spectroscopy could not be employed in this case because the amount of analyte in the solution was very little. Therefore surface enhanced Raman spectroscopy was employed since this technique can successfully produce Raman spectra for very low analyte concentrations. In order to study the ring opening reaction of leflunomide, the reaction was monitored in vitro using NaOH buffer maintaining constant pH ~10. The SERS spectra were recorded at different time intervals after adding the reaction solution to silver substrate.

3. Result and Discussion

3.1 Transition state calculations of isoxazole deprotonation

The conformational stability of leflunomide has been investigated by density functional theory at the B3LYP/6-311++g(d,p) level. Transition state calculations were performed in order to understand the reaction mechanism of metabolite formation of leflunomide through direct proton transfer as well as using water molecule. Fig. 1 presents a schematic comparison between the ring opening mechanism occurring in liver and in-vitro. The optimized structures of leflunomide and its active metabolite A771726 are also shown in Fig. 1. Here we shall consider only some selected aspects of the structure of leflunomide which are relevant to its metabolic process. The benzene group, N-H group and C=O group of leflunomide which are not directly involved in the ring opening phenomenon were neglected (replaced by H atom) and only the isoxazole ring was considered for transition state calculations. Fig. 2(a) shows the structures of reactant complex (RC), transition state (TS), intermediate complex (IC) and product (PC) for the gas phase reaction of this model structure for ring opening through direct proton transfer. The relative energies between the optimized geometries of RC, TS, IC and PC are similar to those obtained considering the full structure of leflunomide. Removal of these groups does not affect the barrier energy (Fig S1, supplementary information). In going from the RC to the first TS (TS1), the isoxazole N-O bond length is increased from 1.402 to 2.588 Å, while the C-N bond is contracted from 1.302 to 1.231 Å. The activation energy for this reaction step predicted at the B3LYP/6-311++g (d, p) level is 45.11 kcal/mol [Fig. 2(a)]. The activation energy is high due to the absence of a catalyst that can facilitate the proton transfer process.

In order to explore the base catalyzed reaction mechanism, transition state calculations were carried out using water, OH^- anion, formate and (formate + 1water) as possible catalysts. The catalysis of deprotonation of the substrate is expected to occur through

a proper positioning of the base [31]. Fig. 2(b,c) shows the structures of RC, TS and PC for the gas phase reaction of isoxazole with formate and OH^-. The C3H bond length of leflunomide is significantly increased on geometry optimization in the presence of each of these catalysts (Table 1). Each of catalysts provide a negative charge in the vicinity of the N-O bond (Fig. 1) that facilitates proton transfer resulting in the N-O bond cleavage at TS1 [Fig. 2(a)].

Activation energies are calculated from the Gibbs free energy differences between the optimized transition states and the optimized reactant complexes. The transition state calculations reveal the following information:

I. In the case of direct proton transfer [Fig. 2(a)] at TS1, the moving proton H4 is located between C3 and N10 atoms, the C3H4 and N10H4 distances being 1.206 and 1.408 Å, respectively. This reaction is predicted to be exothermic as shown by the ZPE-corrected barrier (45.1 kcal/mol) and released (56 kcal/mol) energies at the B3LYP/6-311++g(d,p) level. At the second transition state TS2, the moving proton H28 is located almost midway between N9 and O8 atoms and the N9H28 and O8H28 distances are 1.106 and 1.661 Å respectively. In this case the barrier and released are 22.5 and 26.1 kcal/mol respectively.

II. On using formate as a catalyst, the activation energy corresponding to TS1 predicted at the B3LYP/6-311++g(d,p) level is 13.5 kcal/mol much less than that obtained in the case of direct proton transfer. This barrier energy is further lowered to12.1 kcal/mol on using formate+1water molecule as a catalyst. The overall reaction is exothermic in both cases. The water molecule placed near isoxazole ring plays an important role to stabilize this reaction. At the first transition state (TS1) water molecule is doubly hydrogen bonded with N9 and O10 atoms and corresponding hydrogen bond lengths are 2.195Å and 2.186 Å while the length of hydrogen bond of O-H---N9 type in RC is 1.954 Å. The barrier energy corresponding to TS2 is 25.2 kcal/mol and energy released is 20.1 kcal/mol.

III. On using OH^- anion as catalyst, the isoxazole N-O bond length is elongated from 1.46 to 1.49 Å at TS1. The other bond lengths have intermediate values between those in RC and PC, except for C3-C4, which is longer in TS1 than in either RC or PC. The general shape of the isoxazole ring is retained, as shown by the C-C-N and the C-N-O angles (Table 1). The activation energy corresponding to TS1 predicated at the B3LYP/6-311++g(d,p) level is 2.3 kcal/mol. Between the two transition states TS1 and TS2, an intermediate complex (IC) is formed. The proton removed from C3 site and OH^- result in the formation of water molecule. This water participates in hydrogen bonding with the ring open structure

represented as IC. This IC is more stable than RC by 54.2 kcal/mole of Gibbs free energy. The barrier energy corresponding to TS2 is 3.4 kcal/mol and the energy released resulting in the metabolite like structure is 60.0 kcal/mol.

The presence of OH^- reduces the gas phase activation barrier energy drastically. Hence a proper selection of the basic catalyst can increase the reaction rate. The forthcoming experimental section we have used NaOH as basic medium.

3.2 Experimental

The SERS spectra show significant changes in the peak positions and band shapes of different Raman bands as the reaction proceeds. Signature of ring opening (metabolite formation) is observed after a time interval of about 80 min. The Raman bands of interest to understand the ring opening mechanism are assigned through potential energy distribution. The comparison of experimental and theoretically calculated Raman spectra is shown in Fig. 3. Discussion of the observed Raman bands will be done by dividing the spectra into two wavenumber ranges; 1500-2300 cm^{-1} and 1100-1500 cm^{-1}.

3.2.1 1500-2300 cm^{-1}:

The SERS spectra at different time intervals in this range are presented in Fig. 4. The reaction is initiated after adding the basic pH buffer of NaOH (pH 10) which provides the hydroxyl ions (OH^-) to the medium. These hydroxyl ions catalyze the deprotonation reaction. The negative charge on the OH^- ion pulls the proton attached to the C3 carbon atom of isoxazole ring and provides path for proton transfer to the O9 atom, which initiates ring opening. The path of this proton transfer is also described in our theoretical transition state calculations (Fig. 2).

In this range primarily five Raman bands are observed just after the reaction is initiated (Time 5 min in Fig. 4). Leflunomide is characterized by two prominent carbonyl stretching frequencies ν(C=O) at 1673 and 1695 cm^{-1} which show gradual lower wavenumber shift as the reaction proceeds. This lower wavenumber shift (~12 cm^{-1} after 80 min and further ~9 cm^{-1} in the final spectrum after 420 min) during the reaction can be explained by considering the charge distribution over the O6, C5, C2, C3 and N10 atoms. As the dihedral angle N10-C3-C2-C5 changes from 92.6° in leflunomide to 179.6° in A771726, the charge cloud shifts from C5=O6 towards C3≡N10 via C2 site. Therefore, this lower wavenumber shift in the C=O stretching mode provides evidence of ring opening of leflunomide. This is strongly supported by the theoretically calculated spectra (Fig. 3). The 1624 cm^{-1} and 1610 cm^{-1} bands are assigned as asymmetric deformation in benzene ring in combination with C-C

stretching and N-H rocking in combination with C-C stretching respectively. The 1598 cm^{-1} band has been assigned to C=N stretching in combination with C-C stretching in the isoxazole ring. With the passage of time, this band shows a continuous shift towards higher wavenumber side. As the reaction proceeds, the basic environment favours deprotonation. Due to deprotonation, the bond order in the isoxazole ring changes and results in large blue shift in this band. This supports the formation of C≡N bond as force constant increases with bond order. This peak is further blue shifted with time suggesting the increase in the amount of the metabolite in the solution. A clear signature of formation of A771726 was observed through appearance of C≡N stretching at 2100 cm^{-1} after 80 minutes. Increase in the intensity of 2100 cm^{-1} band with time supports the increase in the concentration of A771726 in the solution with time. This peak is the Raman signature providing confirmation of metabolite formation.

3.2.2 1100- 1500 cm^{-1}:

The SERS spectra at different time intervals in this range are shown in Fig. 5. The band at 1225 cm^{-1} is assigned to C-C stretching in combination with C3-H wagging. This band shifts towards lower wavenumber side by ~5 cm^{-1} after 80 min of initiation of the reaction and by ~26 cm^{-1} in the final spectrum. The main cause behind this large lower wavenumber shift appears to be the deprotonation of the C3-H proton because C-H bond length increases and C-C bond length decreases when the medium becomes basic. This reduces the strength of C3-H bond resulting in red shift of this band. The intensity of the 1391 cm^{-1} band which is assigned to N-C-H bending in the isoxazole ring increases and a new band at 1376 cm^{-1} appears after 80 min of the reaction. This band has been assigned as O-H wagging in combination with C-O stretching vibration. The intensity of this new peak increases with passage of time. These results are in good agreement with the theoretically calculated Raman spectra shown in Fig. 3.

4. Conclusion:

The reaction of isoxazole ring opening of leflunomide was monitored in vitro for the first time using NaOH buffer at pH ~10 in a 10^{-4} M aqueous solution of leflunomide. In the absence of any enzyme, the isoxazole ring can be cleaved easily by a basic reagent. The ring opening is especially facile with the abstraction of the proton from the C3 site. The changes in the Raman band involving C3 atom in isoxazole ring clearly show the N-O bond cleavage through deprotonation of the C3 site. The gradual lower wavenumber shifts in the C=O stretching mode gives clear evidence of ring opening. This is in close resemblance with the

theoretical Raman spectra. A clear Raman signature of ring opening of leflunomide to form A771726 was observed after 80 minutes. The blue shift in isoxazole ring vibrations and appearance of C≡N stretching mode at 2100 cm^{-1} and O-H wagging at 1376 cm^{-1} confirm the metabolite formation at basic pH 10. In order to understand the catalytic action of OH^-, we have calculated the transition state using OH^- as a catalyst. In addition, we have also calculated the transition states for formate and formate + 1water catalyzed isoxazole ring opening to investigate the alternative sources of catalysis for this reaction. Raman spectroscopy in addition to transition state calculations using DFT has thus been able to present a very clear picture of the metabolic pathway underlying this important biological reaction.

Acknowledgement

RKS, DG, and VD are thankful to German Research Foundation (DFG), Germany for financial support. RKS is grateful to AvH Foundation, Germany and DST, India. PS and DG are grateful to the UGC, India for providing Research Fellowships.

References:

1. Davis JP, Cain GA, Pitts WJ, Magolda RL, and Copeland RA. Biochemistry, 1996, 35:1270-1273.
2. Rozman B. J Rheumatol Suppl, 1998, 53:27-32.
3. Rozman B. ClinPharmacokinet, 2002, 41:421-430.
4. Xu X, Williams JW, Bremer EG, Finnegan A, Chong AS-F, J. Biol. Chem, 1995, 270:12398-12403.
5. Xu X, Williams JW, Gong H, Finnegan A, Chong AS-F, Biochem. Pharmacol, 1996, 52:527-534.
6. Kalgutkar AS, Nguyen HT, Vaz ADN, Doan A, Dalvie DK, Mcleod DG, Murray JC. Drug Metab Dispos, 2003, 31:1240-1250.
7. Stiff DD and Zemaitis MA, Drug Metab Dispos, 1990, 18:888–894.
8. Mannens G, Huang ML, Meuldermans W, Hendrickx J, Woestenborghs R, and Heykants J, Drug Metab Dispos, 1993 21:1134–1141.
9. Boucher JL, Delaforge M, and Mansuy D, Biochemistry, 1994, 33:7811–7818.
10. Dalvie DK, Kalgutkar AS, Khojasteh-Bakht SC, Obach RS, and O'Donnell JP, Chem Res Toxicol 2002, 15:269–299.
11. Nakasa H, Komiya M, Ohmori S, Kitada M, Rikihisa T, and Kanakubo Y, Res Commun Chem Pathol Pharmacol, 1992, 77:31–41.
12. Kitamura S, Sugihara K, Kuwasako M, and Tatsumi K, J Pharm Pharmacol, 1996 49:253–256.
13. Jian Yu, James J. Folmer, Valerie Hoesch, James Doherty, James B. Campbell and Doug Burdette, Drug Metab Dispos, 2011, 39:302-311.
14. Jarosław J. Panek, Aneta Jezierska, Krzysztof Mierzwicki, Zdzisław Latajka, and Aleksander Koll, J. Chem. Inf. Model. 2005, 45:39-48
15. D. Vega, A. Petragalli, D. Frenuández and J.A. Ellena, J. Pharm. Sci., 2006, 95:1075-1083.
16. O. Svenson, M. Josefson, F.W. Langkilde, Chemometrics, Intelligent Laboratory Systems 1999, 49:49-66.
17. M. Lee, H. Kim, H. Rhee, J. Choo, Bull. Korean Chem. Soc. 2003, 24(2): 205-208.
18. P. D. I. Fletcher, S. J. Haswell, X. Zhang, Electrophoresis 2003, 24:3239-3245.
19. M. P. Houlne, C. M. Sjostrom, R. H. Uibel, J. A. Kleimeyer, J. M. Harris, Anal. Chem. 2002, 74: 4311-4319.
20. M. Sackmann and A. Materny, J. Raman Spectrosc. 2006, 37: 305–310.
21. L. Delfino, A. R Bizzarri and S. Cannistraro, Biophys Chem, 2005, 113(1):41-51.
22. K. Kneipp, H. Kneipp and J. Kneipp Acc Chem Res, 2006, 39(7):443-450.
23. L. Baia, M. Baia, J. Popp and S, Astilean, J Phys Chem B, 2006, 110(46): 23982-23986.
24. K.K Strelau, T Schüler, R. Möller, W, Fritzsche and J.Popp, Chemphyschem, 2010, 11(2):394-398.
25. A. D. Becke, J.Chem. phys,1993, 98, 5648.
26. C. Lee, W. Yang, R. G. Parr, Phys. Rev. B,1988, 37,785.
27. M.J. Frisch, G.W. Trucks, H.B. Schlegel, G.E. Scuseria, M.A. Robb, J.R. Cheeseman, V.G. Zakrzewski, J.A. Montgomery Jr., R.E. Stratmann, J.C. Burant, S.J. Dapprich, M. Millam, A.D. Daniels, K.N. Kudin, M.C. Strain, O. Farkas, J. Tomasi, V. Barone, M. Cossi, R. Cammi, B. Mennucci, C. Pomelli, C. Adamo, S. Clifford, J. Ochterski, G.A. Petersson, P.Y. Ayala, Q. Cui, K. Morokuma, D.K. Malick, A.D. Rabuck, K. Raghavachari, J.B. Foresman, J. Cioslowski, J.V. Ortiz, A.G. Baboul, B.B. Stefanov,

G. Liu, A. Liashenko, P. Piskorz, I. Komaromi, R. Gomperts, R.L. Martin, D.J. Fox, T. Keith, M.A. Al-Laham, C.Y. Peng, A. Nanayakkara, M. Challacombe, P.M.W. Gill, B. Johnson, W. Chen, M.W. Wong, J.L. Andres, C. Gonzalez, M. Head-Gordon, E.S. Replogle, J.A. Pople, Gaussian 03,Gaussian, Inc., Pittsburgh PA. 2003.

28. R. Dennington II, T. Keith, J. Millam, K. Eppinnett, W.L. Hovell, R. Gilliland, Gauss Veiw 4.1, Semichem, Inc., Shawnee Mission, KS, 2003.
29. A. Rasmussen, V. Deckert J. Raman Spectrosc. 2006, 37:311-317
30. R. Stöckle, V. Deckert, C. Fokas, R. Zenobi Appl. Spectrosc. 2000, 54:1577–1583
31. Jim Na, K. N. Houk, D. Hilvert J. Am. Chem. Soc. 1996, 118: 6462-6471

FIGURE CAPTIONS

Figure 1. **C**omparison of in vitro and in vivo ring opening mechanisms and optimized structures of leflunomide and its active metabolite A771726.

Figure 2. Isoxazole ring opening and proton transfer through the transition state (TS) **(a)** without any catalyst and with **(b)** formate and **(c)** OH^- as catalysts in gas phase obtained at the B3LYP/6-311++G(d,p) level of theory.

Figure 3. Theoretically calculated Raman spectra of leflunomide and its active metabolite A771726 at the B3LYP/6-311++G(d,p) level of theory.

Figure 4. The Raman spectra of leflunomide powder (bottom) and its 10^{-4} M aqueous solution at pH ~10 after adding the NaOH buffer at different time intervals in the range 1500 - 2300 cm^{-1}.

Figure 5. The Raman spectra of leflunomide powder (bottom) and its 10^{-4} M aqueous solution at pH ~10 after adding the NaOH buffer at different time intervals in the range 1100 - 1500 cm^{-1}.

Table 1: Theoretically calculated bond length and bond angle of leflunomide and its active metabolite.

	Leflunomide (Fig. S1)	**Isoxazole ring+ OH^- (Fig 2)**	**Isoxazole ring+ formate (Fig 2)**
		RC	
Bond length (Å)			
C3-H4	1.081	1.173	1.083
C3-N10	1.302	1.303	1.308
N10-O9	1.402	1.467	1.413
O9-C1	1.340	1.343	1.359
Bond Angle			
C1-O9-N10	110.104	107.423	108.573
O9-N10-C3	104.925	105.814	104.891
C3-C2-N10	112.574	110.925	112.936
		TS1	
Bond length (Å)			
C3-H4	1.196	1.216	1.310
C3-N10	1.226	1.300	1.238
N10-O9	2.609	1.490	1.954
O9-C1	1.224	1.339	1.283
Bond Angle			
C1-O9-N10	93.718	106.854	97.958
O9-N10-C3	70.478	105.768	95.952
C3-C2- N10	149.587	110.893	120.919

[1]**Table 2**: Theoretically calculated vibrational frequencies (cm^{-1}) and their assignment for leflunomide in the range 1000-1800 cm^{-1}.

	Wavenumber (cm^{-1})	**PED**
1	1009.69	ρ(H-C1-C11)(43%) + υ(C1-O9)(30%)
2	1026.86	δ_{Δ}(C-C-C)(60%) + υ(C12-C14)(10%) + υ(C12-C13)(11%)
3	1062.07	δ_{as}(H-C1-C11)(67%)
4	1072.18	υ(C22-F25)(20%) - δ(F-F-C11)(14%) - υ(C15-C19)(13%) - υ(C17-C19)(13%)
5	1100.08	υ(C22-F25)(43%) - υ(C22-F23)(13%) + ρ(F-F-C22)(12%) - υ(C22-F24)(10%)
6	1104.06	υ(C5-N5)(20%) - υ(C22-F23)(15%) - δ in isoxazole ring(10%)
7	1122.56	υ(C22-F24)(34%) - υ(C22-F23)(19%)
8	1165.12	υ(C22-F24)(15%) - υ(C22-F23)(19%) + β(C-H18-C14)(11%) - β(C-H21-C17)(10%)
9	1192.81	ρ(C3-H4)(38%) + υ(C2-C3)(27%)
10	1207.36	β(C-H16-C13)(22%) - β(C-H20-C15)(19%) + β(C-H18-C14)(22%) - β(C-H21-C17)(10%)
11	1259.01	ρ(C3-H4)(21%) - υ(C1-O9)(13%) + δ in isoxazole ring(12%) + υ(C1-C11)(11%)
12	1265.63	υ(C12-N7)(26%) + υ(C1-O9)(15%) - υ(C14-C17)(10%) - υ(C12-C13)(10%)
13	1271.09	υ(C1-O9)(19%) + β(C-H8-N7)(12%) - υ(C2-C5)(11%) + υ(C5-N7)(10%)
14	1319.83	υ(C19-C22)(45%) + δ[(F-F-C22)+(F-C19-C22)](18%)
15	1338.32	β(C-H21-C17)(25%) + β(C-H18-C14)(21%) - β(C-H16-C13)(16%) - β(C-H20-C15)(16%)
16	1348.12	υ(C12-C14)(17%) + υ(C17-C19)(17%) - υ(C15-C19)(13%) - υ(C12-C13)(11%) + υ(C13-C15)(10%)
17	1389.12	υ(C2-C3)(24%) - δ[(H-H-C11)+(H-C1-C11)](21%) + υ(C3-N10)(13%) - υ(C2-C5)(12%)
18	1413.69	δ[(H-H-C11)+(H-C1-C11)](69%)
19	1437.12	υ(C14-C17)(21%) - υ(C13-C15)(18%) + β(C-H20-C15)(12%)
20	1467.43	ρ(H-H-C11)(82%)
21	1542.67	β(C-H16-C13)(20%) - β(C-H8-N7)(18%) + υ(C15-C19)(16%)
22	1553.97	β(C-H8-N7)(22%) + β(C-H18-C14)(14%) + υ(C12-N7)(14%) + υ(C17-C19)(12%)
23	1626.16	υ(C1-C2)(31%)
24	1633.53	υ(C17-C19)(13%) + υ(C12-C13)(13%) + υ(C1-C2)(13%) – β(C-H8-N7)(10%)
25	1656.61	υ(C13-C15)(21%) + υ(C14-C17)(17%) + δ_{as}(C-C-C)in benzene ring (10%)υ(C1-C2)(31%)
26	1732.64	υ(C5-O6)(70%)

[1] Abbreviations: ν; stretching, β; bending, ρ; rocking, δs; Symmetric deformation, δas; Asymmetric deformation

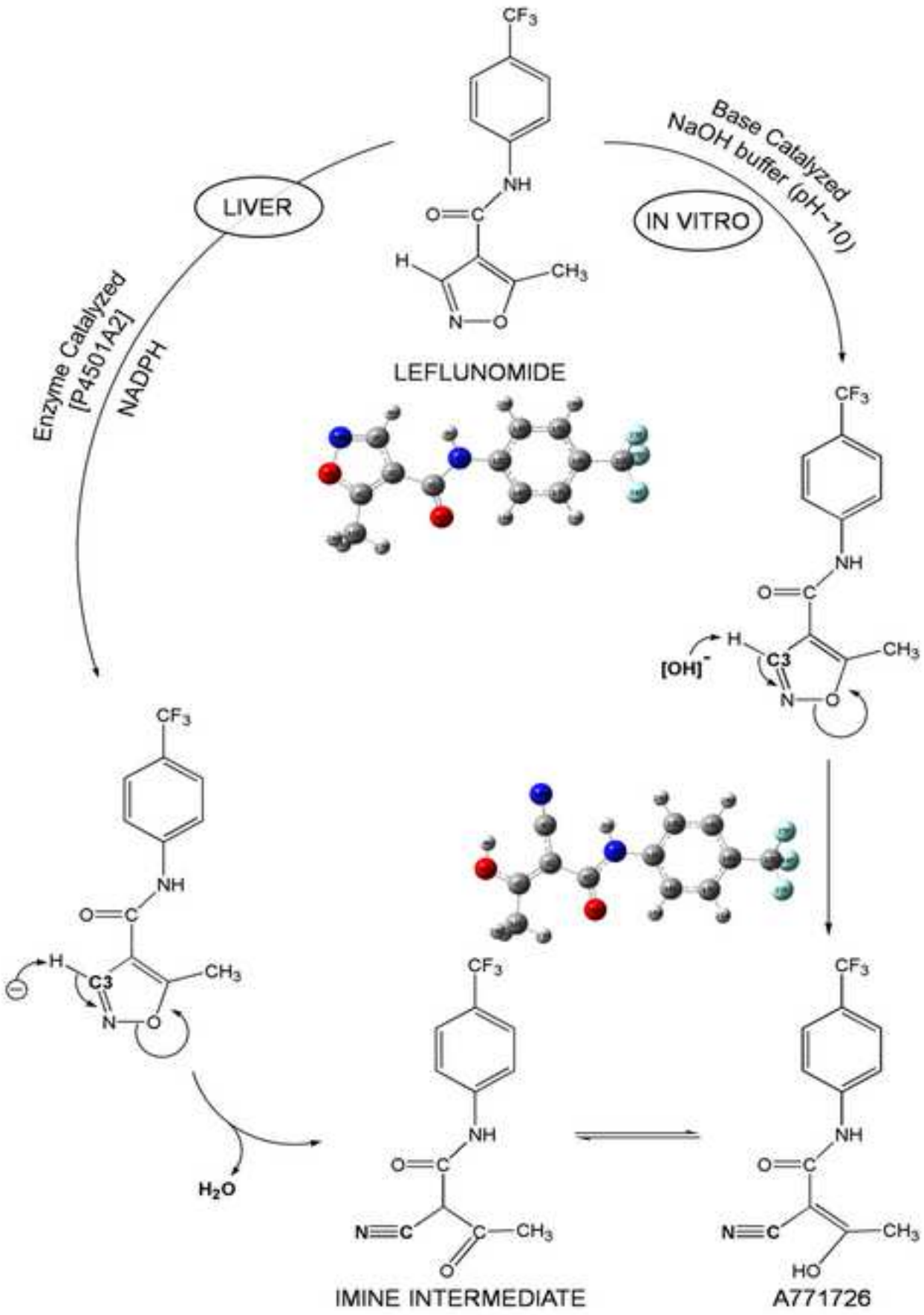

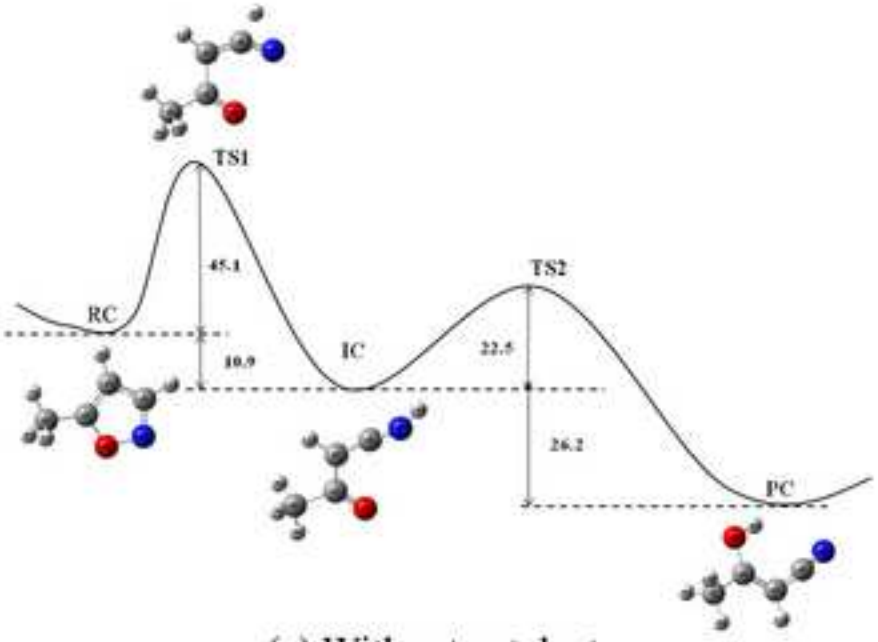

(a) Without catalyst

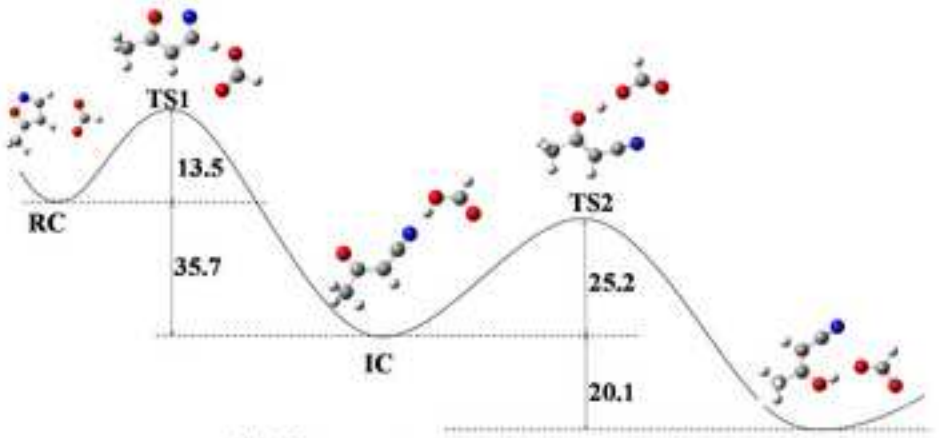

(b) Formate as a base catalyst

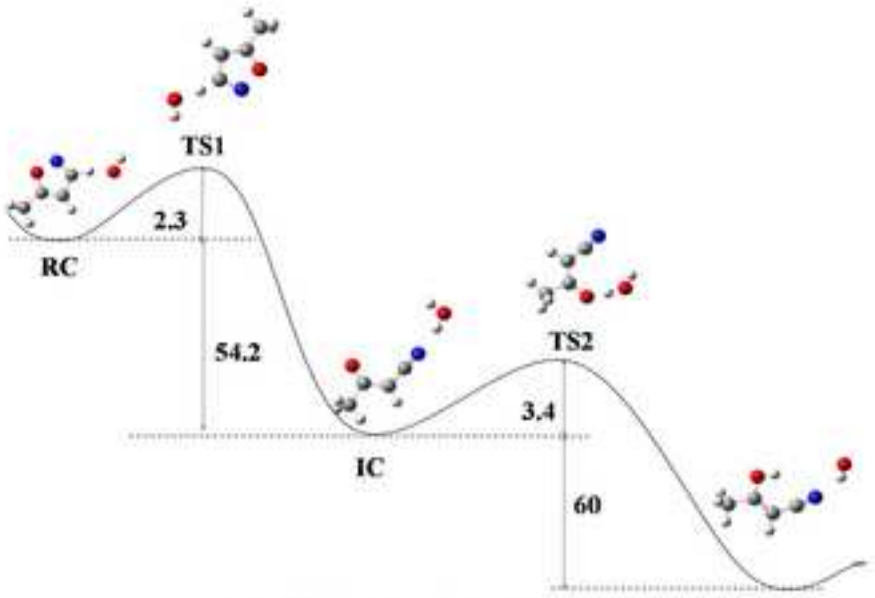

(c) OH^- as a base catalyst

Figure 3

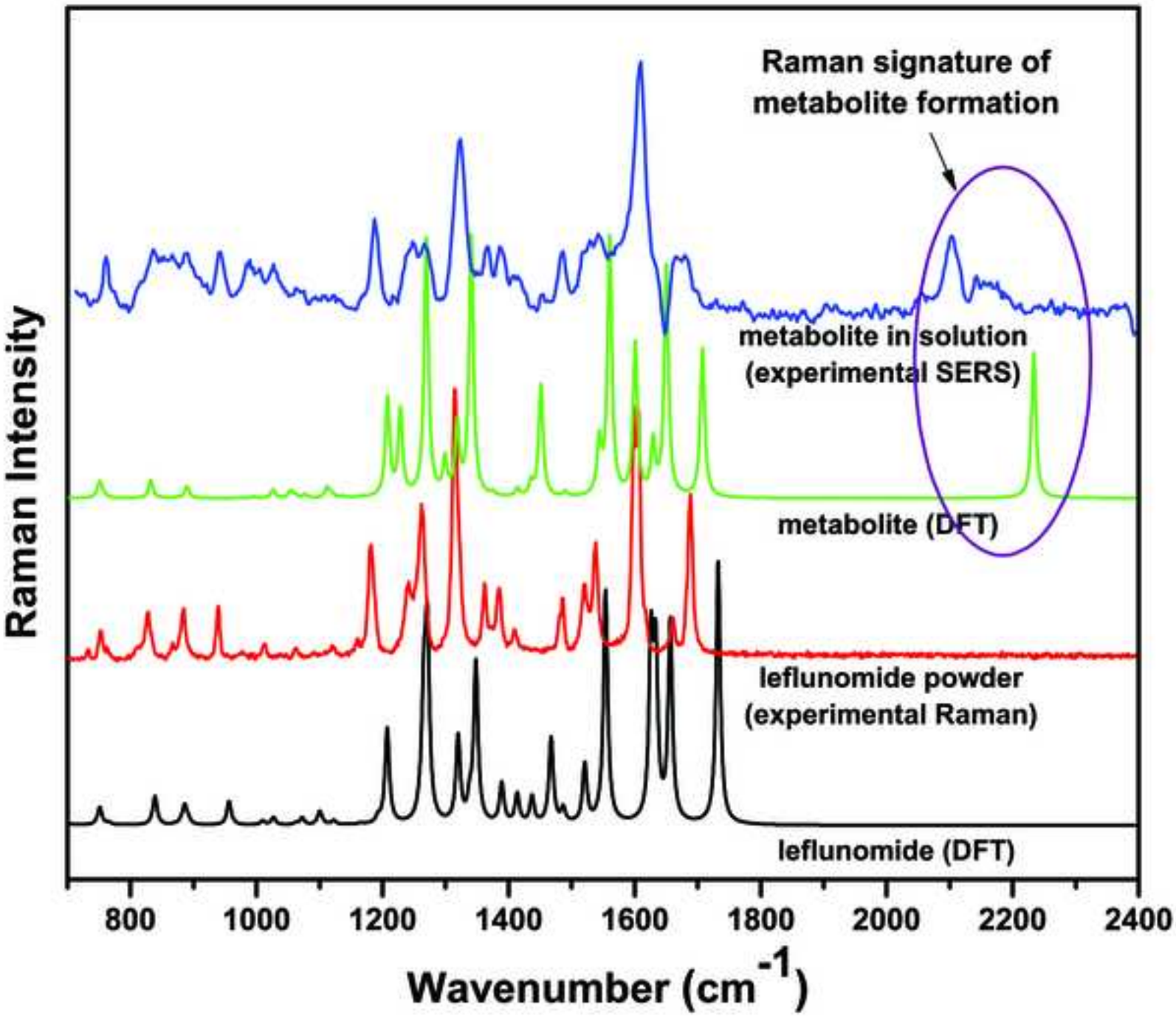
Raman signature of
metabolite formation
metabolite in solution
(experimental SERS)
metabolite (DFT)
leflunomide powder
(experimental Raman)
leflunomide (DFT)
Raman Intensity
800
1000
1200
1400
1600
1800
2000
2200
2400
Wavenumber (cm-1)

Figure 4

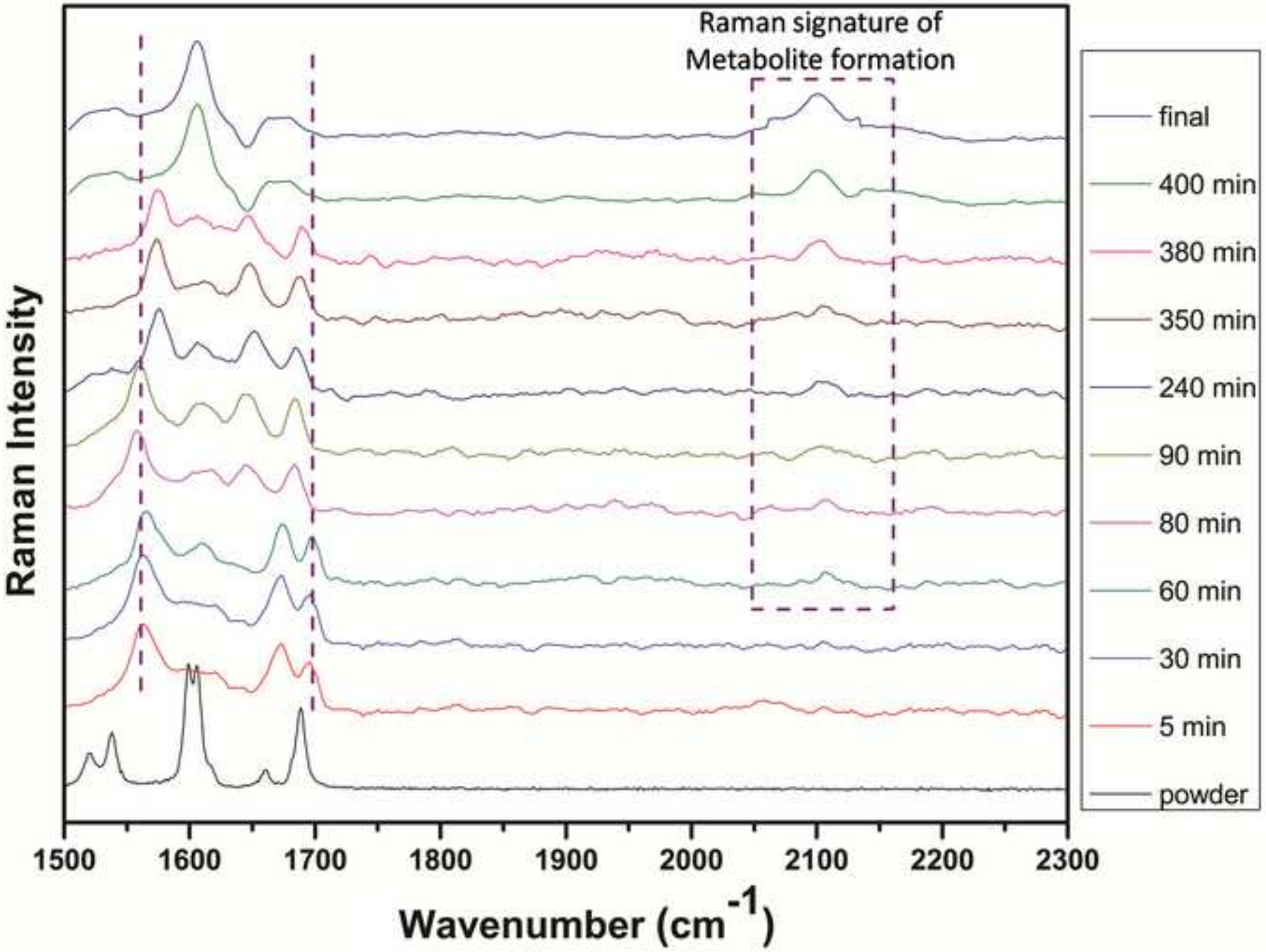
Raman signature of
Metabolite formation
Raman Intensity
Wavenumber (cm-1)
1500
1600
1700
1800
1900
2000
2100
2200
2300
final
400 min
380 min
350 min
240 min
90 min
80 min
60 min
30 min
5 min
powder

Figure 5

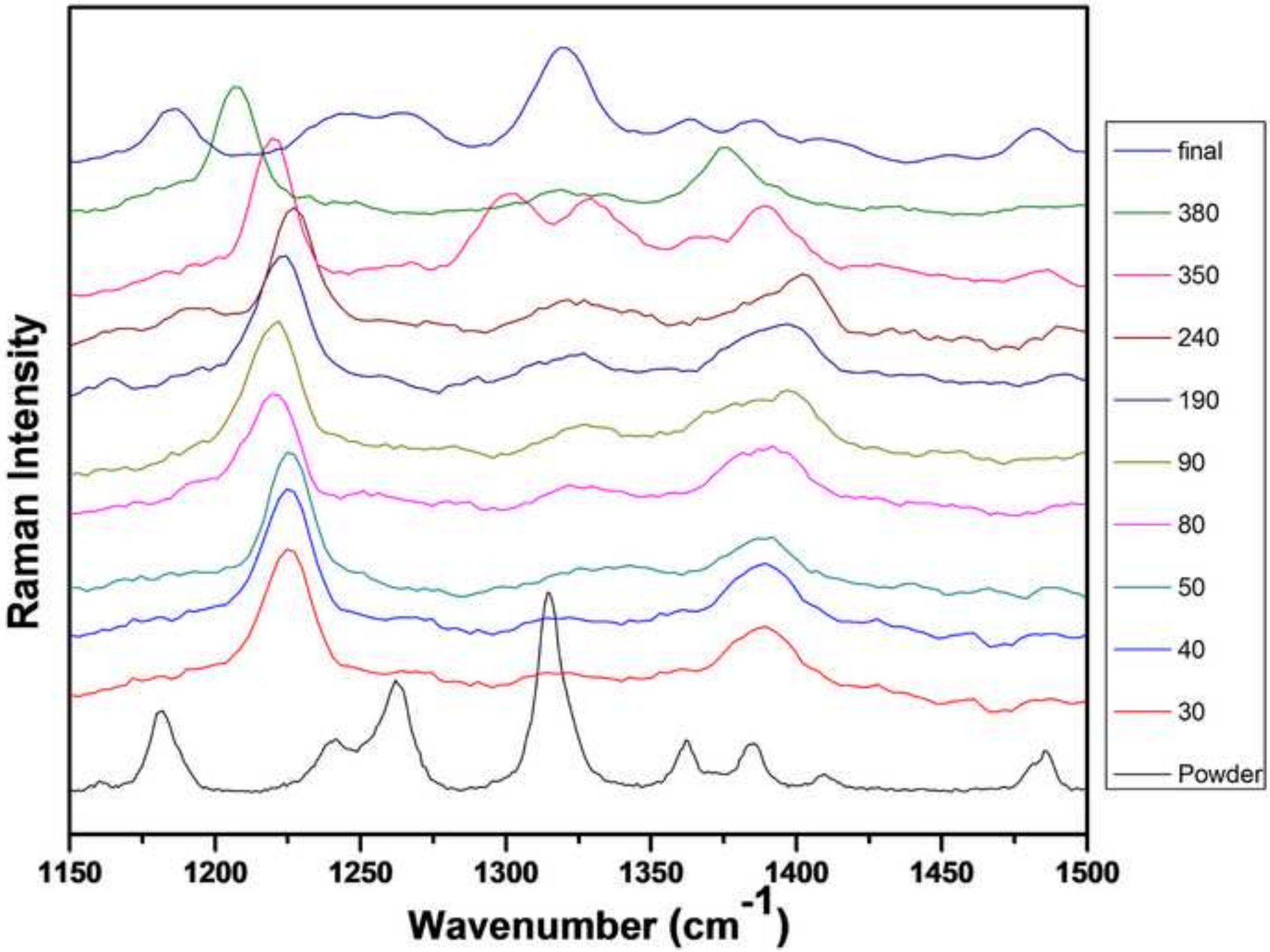
Raman Intensity
1150
1200
1250
1300
1350
1400
1450
1500
Wavenumber (cm-1)
final
380
350
240
190
90
80
50
40
30
Powder